Neutrino signals from neutron star implosions to black holes

Yossef Zenati [*]
Department of Physics and Astronomy, Johns Hopkins University, Baltimore, Maryland 21218, USA

Conrado Albertus [†] and M. Ángeles Pérez-García [‡]
Department of Fundamental Physics and IUFFyM, University of Salamanca, Plaza de la Merced S/N E-37008, Salamanca, Spain

Joseph Silk [§]
Department of Physics, University of Oxford, Keble Road OX1 3RH, Oxford, United Kingdom; Institut d'Astrophysique, UMR 7095 CNRS, Sorbonne Université, 98bis Boulevard Arago, 75014 Paris, France and Department of Physics and Astronomy, Johns Hopkins University, Baltimore, Maryland 21218, USA

(Received 17 April 2023; revised 4 November 2023; accepted 24 February 2024; published 13 March 2024)

We calculate the neutrino luminosity when dark matter is captured by a neutron star that eventually implodes to form a low-mass black hole. A central disk forms out of the ejected material with a finite radial extension, density, temperature, and lepton fraction, producing fainter neutrino luminosities and colder associated spectra than expected in regular core-collapse supernova and black hole–neutron star mergers. The emitted gravitational wave signal from the implosion should be detectable with ultrahigh-frequency resonant cavities in the range ∼0.1–1 GHz.

DOI: 10.1103/PhysRevD.109.063015

I. INTRODUCTION

Massive stars, larger than about $\sim 8 M_\odot$ have short lifetimes and end in core-collapse supernova (CCSN), leaving behind a high-mass neutron star (HNS) or stellar black hole (BH). An important diagnostic is the rate of neutrinos traveling from the inner regions of the core of the massive star and reaching to the stellar surface. Neutrino physics is still under investigation in all areas of astrophysics and fundamental physics itself, including neutrino-matter interactions, energy, momentum, and lepton number transport, and flavor conversion [1]. Neutrinos can change their flavors during propagation, affecting the final yield and elements formed in the ejecta or in the outflow both in CCSN events and in binary NS (BNS) mergers, as known from the recent kilonova event AT 2017gfo, compatible with a BNS merger event at 40 Mpc [2] (see [3–5]) arising ∼0.5 days after the gravitational wave (GW) emission GW170817.

More than five decades after the detection of the first pulsar [6], basic properties of NSs such as their masses and radii are still uncertain [7]. Understanding the features of the M-R curve for NS is key to setting constraints on the high-density part of the matter equation of state (EOS) and the resulting massive objects left in mergers of NS, for example, via GW analysis [8]. Missions such as current LVK detectors—LIGO Livingston, LIGO Hanford, Virgo, and KAGRA—the Einstein Telescope (ET) [9] in Europe, and Cosmic Explorer (CE) [10] in the United States will be able to test strains $\mathrm{Log}(\mathrm{h}[1/\sqrt{\mathrm{Hz}}]) \gtrsim -26$. Recent studies [11] considering two different detector configurations have analyzed detection prospects for BNS that could reshape our understanding of the underlying EOS from parameter estimation for simulated events. Based on the uncertainties on the tidal deformabilities associated with these events, one can extract the underlying injected EOS within a Bayesian framework. Remarkably, it is claimed that, with $\gtrsim 500$ events, one could have detections with signal-to-noise ratio SNR $\gtrsim 12$, allowing the possibility of precisely pinning down the underlying EOS governing the NS.

Regarding composition, the interiors of these objects can be described in terms of a screened ionic lattice in the crust [12] and a deeper hadronic core but remain yet poorly known. Analogously, from seminal papers [13,14], there is now a vast literature about the possibility that matter of a different nature, yet unknown, but with feeble interactions with Standard Model particles, can clump in the Universe and populate astrophysical bodies.

The evidence for dark matter (DM) is currently overwhelming, ranging from galaxy rotation curves,

[*] yzenati1@jhu.edu
[†] albertus@usal.es
[‡] mperezga@usal.es
[§] silk@iap.fr

gravitational lensing, cosmic microwave background, and more [15]. Concerning the zoo of current DM candidates in the dark sector, there are some which are especially popular, such as weakly interacting massive particles [16], axions (or axionlike particles), [17] and primordial BHs (PBHs); see [18] for a review.

PBHs are generated by inflation due to tailored primordial fluctuations and can explain all of the DM in some mass windows [19]. Note that, from current constraints, there is a possibility that a fraction of DM is in the form of PBHs coexisting with additional particle candidates. Determining the optimal PBH mass window remains problematic and is highly constrained from recent GW detections associated with binary BHs in the mass range $10-50M_{\odot}$ and by gravitational microlensing experiments over the mass range $\sim(10^{-9}\text{–}10^{2})M_{\odot}$.

We focus on the interface of dense clouds of DM, NS, and BH. In dense clouds of DM, the NS can accrete a significant amount of it so that gravitational collapse may be triggered. The effect is especially strong if the DM is asymmetric, also known as non-self-annihilating [20–22]. An alternative pathway to NS collapse is via capture of a PBH [23] as we detail below. The question we address here is how can we test the remarkable scenario of induced NS collapse.

There is wide agreement about how stellar BHs are formed via CCSN as the core engine runs out of exothermic fusion reactions, no longer being able to stop the gravitational contraction. This fate arises above the NS mass upper limit, currently at $M_{\max} \geq 2.01M_{\odot}$ [24].

In 2019, it was reported [25] that the GW190814 event was consistent with a binary BH merger where the lightest object $\sim 2.6M_{\odot}$ was most likely in a mass gap roughly in the range $\sim(2\text{–}5)M_{\odot}$. In addition, recent analysis using Hubble Space Telescope archival data and densely sampled light curves from ground-based microlensing surveys has spotted OB110462, that is an isolated BH with an inferred lens mass $\sim 1.6\text{–}4.4M_{\odot}$ [26].

An alternative scenario is that where a low-mass BH may form from the induced collapse, also referred to in the literature as transmutation, of a NS due to the accretion of DM. At this point, it is important to emphasize that different dark agents may trigger this transformation as has been recently discussed in the literature; see [27]. Just to cite some examples, accretion of critical numbers of fermionic or bosonic DM particles can induce the growth of an internal self-gravitating BH [21,28–30]. Capture or transit of a PBH may also trigger the catastrophic event [31–33]. Yet this collapse may also be induced by a dramatic lowering of pressure from the nucleation of quark bubble instabilities [34,35] and caused by self-annihilating DM in the so-called *Trojan horse* mechanism. Note, however, that our interest in this work is in evaluating the common or expected neutrino signal after the induced collapse, according to the previous scenarios or any others that might happen. Elucidating between these scenarios may involve peculiarities that are beyond the scope of this work.

The induced implosion of the NS has been shown to produce multimessenger emission, mostly electromagnetic (EM) transients [36] or cosmic rays [37,38]. These transients are not accompanied by significant gravitational radiation or neutrinos, allowing such events to be differentiated from compact object mergers occurring within the distance sensitivity limits of GW observatories; see [39,40].

The actual rate estimated for these events is largely unknown, as in our scenario it depends on the dark environmental conditions. Whatever the candidate is to DM, there is accretion onto the NS, for example, under the PBH hypothesis, when it collides with NS perhaps in the optimal environment, namely, the Galactic Center, where it accumulates DM [41,42]. One of the critical parameters for the estimation of collision rates is the typical distance between objects. Lastly, there is not a broad consensus about the observed signatures in the PBH mass range. In the scenario presented here, there will be a multimessenger signal from the NS implosion. The local rate of NS formation, estimated as the local rate of CCSN, gives an upper limit for the rate of NS conversions, on the order of [43] $\mathcal{R}_{\mathrm{NSimplosion}} \lesssim 1.01 \times 10^{5}\ \mathrm{Gpc}^{-3}\,\mathrm{yr}^{-1}$. Other distinctive features, such as emission of a very short gamma-ray burst [36], were found to be dependent on beaming factors $\langle f_b \rangle$ when averaged to $\mathcal{R}_{\mathrm{NSimplosion}} \sim 10^{-3}(\langle f_b \rangle/50)\ \mathrm{Gpc}^{-3}\,\mathrm{yr}^{-1}$. Focusing on our Galaxy, the capture rate of a tiny PBH by a NS was reduced to [32,33] $\sim 10^{-10}\ \mathrm{Gpc}^{-3}\,\mathrm{yr}^{-1}$. Hitherto the uncertainties remain large, as in the alert [44] on possible "quiet kilonovae," i.e., those not accompanied by the significant GW signal of a BH-NS or BNS merger and pointing toward the possibility of elucidating such rates through the complementary abundance of r-process material.

II. DARK MATTER INSIDE AN ISOLATED NS

In a regular NS with ordinary matter EOS $P(\rho)$, the static or rotating solution of the stellar structure equations in the general relativistic framework predicts the mass-radius (M-R) curve where compact stars can exist in stable configurations [45] up to a maximum mass. For isolated NS, with $M \lesssim 2.2M_{\odot}$, it is unlikely that a BH is formed, according to the usual scenario. However, several novel mechanisms involving DM have been studied that could distort, in principle, the stellar stability. As an example, let us consider the presence of asymmetric dark matter (ADM) inside the NS. As studied by several authors, DM in the form of massive particle candidates could be gravitationally captured and accumulated in the NS core [46,47] in sufficient numbers to trigger the gravitational collapse once a dark critical mass (or particle number $N_{\chi,\mathrm{crit}}$) is reached [48,49].

An interesting scenario intimately related to this concerns a PBH colliding with a NS [50–52], since a possible high signal-to-noise measurement could demonstrate the existence of light BHs produced in these collisions. In a binary including a light BH, this involves inspiral and merger phases, in which component masses lie well within the NS mass range. Abramowicz *et al.* [53] claim that GW detectors and microlensing are, in principle, capable of detecting such objects. Special attention has been devoted to recent sub-solar-mass PBH searches [54] with Advanced LIGO and Advanced Virgo using coalescing binaries. The bosonic or fermionic nature assumed for the dark sector would not change the basic picture as presented here. In the case of self-annihilating DM, the Trojan horse mechanism [34,55] of efficient spark injection producing quark nucleation in the core of the NS may lead to long-hypothesized quark star formation and subsequently BH.

We start from a treatment where ordinary matter and DM interactions are essentially gravitational with a simplified two-fluid formalism. An admixed star with ordinary matter (fluid 1) and generic DM candidates χ (fluid 2) displays a M-R curve that shows different maximum masses allowed for baryonic and dark overlapping distributions as obtained from solving the structure equations.

It has been found [21] that, for particle ADM candidates with mass above a value $m_\chi = 10^8$ GeV, there are admixed NS solutions that yield the maximum mass around the threshold $\sim 1 M_\odot$ so that, beyond this value, collapse to a BH would follow [22].

Typically, a massive NS with mass M and radius R is born with a rotation frequency ω less than the Keplerian frequency value Ω_K being dependent on the precollapse object as shown by recent work [56]. Studying the effect of Ω on a fluid element with angular velocity relative to that of the local inertial frames $\omega(r)$ in rotating NS shows

$$\Omega_K \simeq \left[1 + \frac{\omega(R)}{\Omega_K} - 2\left(\frac{\omega(R)}{\Omega_K}\right)^2\right]^{-0.5} \left(\frac{GM}{R^3}\right)^{0.5}, \quad (1)$$

so that, using the relevant solution of the Einstein equations, one can approximate [57]

$$\Omega_K \sim 0.65(GM/R^3)^{0.5}. \quad (2)$$

Briefly, our 1D hydro general relativity code is based on the evolution equations for the hydrodynamic variables using a second-order ordinary differential equations (ODE) scheme; see Secs. 2.2 and 2.1 in [58,59], respectively. This includes radial gauge, polar slicing metric

$$g_{ab} = \mathrm{diag}(-\alpha^2, X^2, R^2, R^2 \sin\theta^2), \quad (3)$$

with $X = (1 - 2m(r)/r)^{-0.5}$ and $m(r)$ is solved from an ODE for the enclosed gravitational mass, i.e.,

$$dm/dr = 4\pi(\rho h \gamma^2 - P + \tau^\nu_m), \quad (4)$$

with $m(0) = 0$. The ${\tau^\nu}_m = 0$ is part of the gravitational mass from the energy and pressure of trapped matter. The enthalpy is given by

$$h \equiv 1 + \epsilon + P/\rho \quad (5)$$

and the Lorentz factor $\gamma \equiv (1 - v^2)^{-0.5}$, where global units are used $G = c = M_. = 1$. In addition, the relation

$$\omega(R)/\Omega_K = 2I/R^3 \quad (6)$$

is fulfilled, I being the stellar moment of inertia. Although correlation effects in rotating NS regarding different EOS and the effects on the stellar structure are indeed possible, this is out of the scope of this work.

III. NEUTRINO EMISSION

To model the disk surrounding the BH, we consider electrically neutral matter with electrons (e^-), muons (μ^-), protons (p), and neutrons (n) in the baryon (b) sector which are to good approximation consistent with the thermodynamical conditions ρ, T assumed in the scenarios explored. As a specific realization, we adopt the polytropic EOS of dense matter APR and PPEOS [60,61], which fulfills the minimum constraint of producing M-R curves with maximum NS mass value beyond $2M_\odot$. We initialize the electron fraction Y_e by the initial condition of neutrino-free beta equilibrium $\mu_\nu(\rho, Y_e, T) = 0$, where μ_ν is the neutrino chemical potential. As mentioned in the introduction, we do not discuss in what follows specific features of alternative NS implosion scenarios, as we will focus in the physical situation when the collapse has been already triggered and the disk is formed around the existing BH.

The disk surrounding the BH formed from the debris of the NS implosion can be described in terms of an electron fraction or ratio of electron to baryon number densities in the form $Y_e = n_e/n_b$. We will assume baryon number conservation so that proton and neutron number densities fulfill the relation

$$n_b = n_p + n_n, \quad (7)$$

and electrical charge neutrality in matter involves

$$n_e + n_\mu = n_p, \quad (8)$$

n_μ being the muon number density. Assuming matter is in weak equilibrium, the following reactions hold: $n \leftrightarrow p + e^- + \bar{\nu}_e$ and $\mu^- \leftrightarrow e^- + \bar{\nu}_e + \nu_\mu$. As a consequence, particle population balance can be expressed from chemical potential relations $\mu_p = \mu_n - \mu_e$ and $\mu_\mu = \mu_e$ for neutrinos escaping the site. No heavier species are involved. The specific form for the previous expressions regarding charge

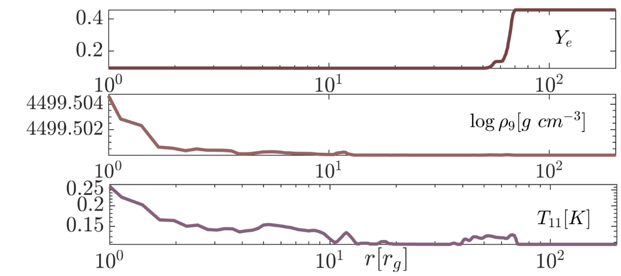

FIG. 1. Top to bottom: electron fraction, mass density normalized to 10^9 g/cm^3, and temperature normalized to 10^{11} K as functions of radial coordinate in r_g units at $t = 1$ ms after the collapse event. Note that the system isospin symmetry is recovered beyond a distance $\sim ct$.

conservation is determined by the degree of lepton and nucleon degeneracy $\eta_i = \mu_i/T$, $i = e, \mu, p, n, \nu$, i.e., the chemical potential-to-temperature ratio of each species in the system.

Figure 1 shows some quantities of interest as functions of the radial coordinate for (ordinary) matter beyond the horizon as given from the Schwarzschild BH radius $r_g = 2GM/c^2$. We show (from top to bottom) electron fraction, Y_e, mass density ρ normalized to 10^9 g/cm^3, and temperature T normalized to 10^{11} K at $t = 1$ ms after the collapse event (see [62,63]). Neutron-rich matter at densities 10^{11-12} g/cm^3 is present for distances $[1, 60]r_g$ to the BH, while it is isospin symmetric beyond a distance $\sim ct$. Similarly, T decreases slowly with larger r with an average value around $\sim$1 MeV.

Our numerical scheme calculates the absorption or emission rate as well as the energy-loss rates due to neutrinos. Specifically, we consider β processes with electron-positron capture rate by nucleons $e^- + p \to n + \nu_e$, $e^+ + n \to p + \bar{\nu}_e$, plasmon decay, where quanta of EM field in a plasma, i.e., photons (γ) lead to neutrino-antineutrino pairs, $\gamma \to \nu_e + \bar{\nu}_e$, $\gamma \to \nu_x + \bar{\nu}_x$, where x denotes generically the μ and τ flavors. We also consider electron-positron pair annihilation rate, $e^- + e^+ \to \nu_e + \bar{\nu}_e$, $e^- + e^+ \to \nu_x + \bar{\nu}_x$, and the nucleon-nucleon bremsstrahlung rate, $N + N \to N + N + \nu + \bar{\nu}$.

Figure 2 (left) shows the neutrino emissivities in the disk, $\bar{q}$ (per unit volume), as a function of radial distance (in r_g units) for the different processes considered in our calculation, i.e., nucleon-electron (positron) Ne, electron-positron pair annihilation, e^+e^-, NN bremsstrahlung, $NN_{\rm Brems}$, and plasmon decay γ, up to $r \sim 7r_g$. Figure 2 (right) shows the spherical differential neutrino luminosity for $\nu_e, \bar{\nu}_e, \nu_x$ ($x \equiv \mu, \tau$ flavors) from the BH formation site up to the radial coordinate $r = 100r_g$ at $t = 1$ ms after the collapse with initial magnetic field $B = 0.5B_{16}$, where $B_{16} = 10^{16}$ G. For these B intensities, the matter results in being only slightly spin polarized, and neutrino dynamics do not change significantly [64]. The neutrino luminosity is large for all neutrino flavors close to the BH and quickly fades by 3 orders of magnitude in the external disk regions, this effect being more dramatic for x flavor. One crucial process of neutrino absorption by nucleons, $\nu + n \to e^- + p$, provides the main channel for the scattering optical depth.

Neutrino luminosities are shown in Fig. 3 (left) as a function of time from the BH formation site. They are compared to limiting cases (dashed lines) from a regular CCSN progenitor in the mass interval $[9.6, 18]M_\odot$ [65] and those from BH-NS merger accretion disk as obtained in unmagnetized accretion disks in [66] for initial masses of the BH and NS being 7 and $1.2M_\odot$, respectively [66]. In more detail, we show specific cases for flavors ν_e, $\bar{\nu}_e$, and ν_x (in units of 10^{51} erg s^{-1}) evolving with time after bounce (in seconds) of the prompt collapse for $1M_\odot$ (solid line) and $2M_\odot$ (dashed line) BH in Fig. 3 (right).

Let us note that the evaluation of neutrino luminosities involves a gravitationally redshifted volume element when integrating neutrino emissivities [67]. These $\mathcal{O}(1)$ factors due to nonflat space-time will hardly modify the order of magnitude numerical values obtained roughly as

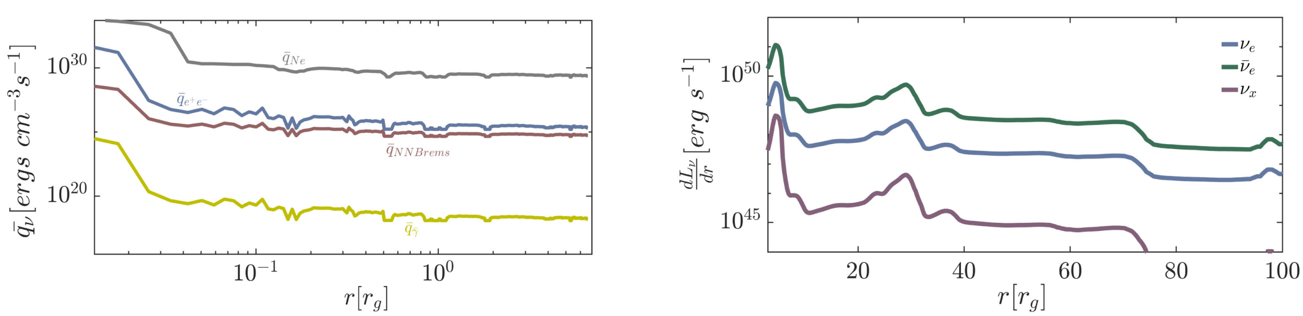

FIG. 2. Left: neutrino emissivities per unit volume in the disk as a function of radial distance (in r_g units) for the different processes considered, i.e., nucleon-electron (positron) Ne, electron-positron pair annihilation e^+e^-, NN bremsstrahlung, NN $Brems$, and plasmon decay (γ) up to $r = 10r_g$. Right: differential luminosity due to neutrino species $\nu_e, \bar{\nu}_e, \nu_x$ as a function of radius in r_g units at t = 1 ms after the NS collapse with initial $B = 0.5B_{16}$, where $B_{16} = 10^{16}$ G.

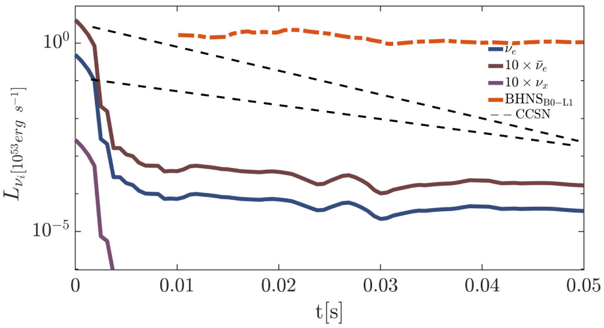

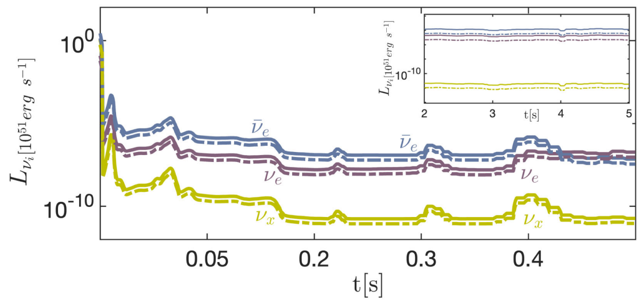

FIG. 3. Left: time evolution of neutrino luminosities (units of 10^{53} erg s^{-1}) after collapse and $M_{\mathrm{BH}} = 1M_{\odot}$ formation, for flavors ν_e, $\bar{\nu}_e$, and ν_x. We show the limiting curves for cases $[9.6, 18]M_{\odot}$ CCSN [65] and those in the BH-NS merger event as obtained in unmagnetized accretion disks in [66] for initial masses of the BH and NS being 7 and $1.2M_{\odot}$, respectively. Right: the neutrino luminosities for flavors ν_e, $\bar{\nu}_e$, and ν_x (units of 10^{51} erg s^{-1}) evolution with time after bounce (seconds) of the prompt collapse of NS to BH driven by DM capture. The solid and dashed line elucidate $M_{\mathrm{BH}} = 1M_{\odot}$ and $M_{\mathrm{BH}} = 2M_{\odot}$, respectively.

$$L_{\nu} \sim \int \bar{q}_{\nu} dV. \tag{9}$$

A similar comment follows regarding the redshift effect on photon luminosity, obtained as

$$L_{\gamma} \sim 4\pi R^2 \sigma T^4, \tag{10}$$

with σ the Stefan-Boltzmann constant.

We find that, in most of the emission cases analyzed, the neutrino luminosity associated with the NS implosion creating the BH will be systematically fainter than regular CCSN or predictions for BHNS coalescence such as in the generic example of unmagnetized accretion disks in [66], respectively. Thus, for distant events, a few neutrinos may reach detectors on Earth such as SuperKamiokande, ANTARES, or IceCube. Although neutrinos from catastrophic implosion events or binary mergers could open a new window for multimessenger research by looking for coincidence signals at times around GW detections, it seems technically very challenging. Several coincidence searches have been performed for GW150914, GW151226, and GW170817 using a wide energy range from 3.5 MeV to 100 PeV. The SuperKamiokande analysis was performed within a time window of ± 500 s, as well as 14 days after the events, finding only neutrino events compatible with the background [68,69] within distance of 260 kpc at 90% C.L. Similar null results are reported from more recent data [70,71].

A. Gravitational wave strain

Below, we discuss how the NS implosion is expected to be associated not only with bursting neutrino and EM emission, but with a transient GW signal, and we roughly estimate its magnitude. Most of the EM energy is radiated away on dynamical timescales, giving rise to another correlated transient signal, as shown in [36]. Refined GW calculations are beyond the scope of this work and will be published elsewhere.

As the NS accretes DM (fluid 1) from capture or transit of external entities, the host star consisting of mostly ordinary matter (fluid 2) develops spatial distributions inside, $\rho_1(r)$ and $\rho_2(r)$, respectively, that may finally lead to the NS implosion. Apart from the expected multimessengers in the form of photons and neutrinos, GW emission is also expected in this catastrophic event. To our knowledge, no numerical simulations have been performed regarding the likely off-center DM nucleation trigger and subsequent NS collapse.

For an old NS collapse induced by accretion of fermionic or bosonic DM component, there is a critical number of particles for triggering the NS transition to $\sim M_{\odot}$ BH that can be estimated as

$$N_{\chi}^{\mathrm{crit}} \simeq 6 \times 10^{26} \left(\frac{10^{15}\ \mathrm{g/cm^3}}{\rho_c}\right)^{1/2} \left(\frac{T}{10^5\ \mathrm{K}}\right)^{3/2} \times \left(\frac{10^8\ \mathrm{GeV}}{m_{\chi}}\right)^{5/2}, \tag{11}$$

where ρ_c is the ordinary matter central density and we assumed ADM particle mass $m_{\chi} \sim 10^8$ GeV; for additional parameter space, see Fig. 1 in [21]. However, if the DM candidate is self-annihilating, a seeding mechanism may lead to collapse for smaller critical masses [34,35].

It is beyond the scope of this work to compute the transient accurate GW signal of the NS implosion. Even for other transient emission such as for BNS [72], continuous GW as expected for NS glitches [73], or a hypothesized hadron-quark deconfinement phase transition [74], it remains a challenging task. Because of the complexity and nonexistence of transient waveforms and in order to estimate the strength of the GW signal, expected to be weak for nonbinary compact object mergers, we assume, in line with [75], that the collapse process is not fully axisymmetric and, as a result, the $l = m = 2; l = 2, m = 0$ spherical harmonic components contribute to the quadrupole moment and waveform emitted. The former arises from the evolution of the quadrupole moment during the collapse process, and the (2, 0) component comes from the collapsing, angular-averaged remnant, which is nonspherical due to its spin. The imploding NS develops a transient disk from angular momentum considerations. Hence, the collapsing system develops a quadrupole moment [see Eq. (14)] during the NS implosion due to DM accretion.

There are several sources for triggering GW emission in the processes expected from internal instabilities and deformation in the NS implosion. Since the complex physics of the event is out of scope in this work, we will consider a more tractable example, sharing some similarities; for the sake of discussion, let us consider transient deformations such as NS glitches. These can be modeled as rectangular or decaying exponential signals (with finite duration) with maximum strength h_0.

In our assimilated picture, the transient duration of the total GW energy emitted $E_{\rm GW}$ lies naturally in the asymmetric DM mass triggering the collapse in the unconstrained PBH mass gap $m_{\rm PBH} \in [10^{-16}, 10^{-12}]M_\odot$ and of frequency $f_{\rm GW}$ during a dynamical time scale $\tau_{\rm GW}$. This allows us to infer [73,76]

$$h_0 = \frac{1}{\pi d_L f_{\rm gw}} \left(\frac{5G}{c^3} \frac{E_{\rm GW}}{\tau_{\rm GW}} \right)^{1/2}, \tag{12}$$

where d_L is the distance to the collapsing NS, typically clustering in the Galactic Center,

$$h_0 = 6.0 \times 10^{-25} \left(\frac{8\ \text{kpc}}{d} \right) \left(\frac{E_{\rm GW}}{10^{-16} M_\odot c^2} \right)^{1/2} \times \left(\frac{1\ \text{kHz}}{f_{\rm GW}} \right) \left(\frac{1\ \text{ms}}{\tau_{\rm GW}} \right)^{1/2}. \tag{13}$$

We note that typical estimates for NS glitches are at strain $h_0 \sim 10^{-24}\ 1/\sqrt{\text{Hz}}$, below current sensitivity bounds for on-line LVK interferometer experiments, the CE and ET being the most likely suited for detection in the future. Other works [77] consistently obtain a strain from the radial oscillations triggered in the NS collapse to the BH from the velocity and mass of the asymmetric component of the collapsing matter, v_m and m_m, respectively. Adopting typical infall velocity $v_m \approx 0.1c$ and assuming that m_m is determined by a fraction of the critical DM mass $m_m = f_\chi m_\chi N_{\chi,\rm crit}$ with $f_\chi \sim 0.01$ contributing, typically at the percent level of the mass of the DM inner core. This component is concentrated in regions of typical size $r \sim$ few cm. Thus, naturally $f_{\rm GW} \sim v_m/r$ yields an expected emission range [0.1, 1] GHz. From this, a rough estimate reads

$$h \approx 2.8 \times 10^{-23} \left(\frac{d}{8\ \text{kpc}} \right)^{-1} \left(\frac{m_\chi}{10^8\ \text{GeV}} \right) \left(\frac{v_m}{0.1c} \right)^2, \tag{14}$$

which contributes to the GW emission with strengths accessible only to the sensitivity of current on-line LVK detectors in the 0.01–1 kHz range. However, if the fraction of matter involved in the asymmetric collapse is much smaller or the DM candidate is not so massive, as predicted for bosonic candidates that efficiently trigger low-mass BH formation, the strength may dramatically fall below current limits.

In view of similar results from other candidates, such as PBHs [78], an additional characteristic feature could lead to identifying the transmuted origin of low-mass BHs from the redshift dependence of their merger rate.

Corresponding in this ADM setting to $m_\chi \sim 1$ TeV, lighter DM triggering collapse would not be feasible to detect these weak signals. Furthermore, some studies [79] have shown promising results on subsolar mass BHs performing extreme mass-ratio inspirals around a supermassive BH and SNR in the range of detectability by LISA or ET.

Given the large uncertainties from the lack of reliable simulations, it is worth pointing out here that some estimates [44,80] find instead different GW range frequencies $f_{\rm GW} \lesssim$ 10 kHz emitted for alternative scenarios involving the NS collapse, showing thus the challenging task to obtain a template bank for these events, allowing detection from matched filtering, i.e., comparing the observed data with a set of templates of the expected waveform.

Note that these previous estimates predict different frequency ranges for the expected emission, with modes in the low- and ultrahigh-frequency range. Also for the later case, as claimed in [81], this is characteristic of additional scenarios such as mergers of PBHs in the light-mass range. In this scenario, the predicted strain amplitude is tiny:

$$h_0 \simeq 9.77 \times 10^{-34} \left(\frac{f_{\rm GW}}{1\ \text{GHz}} \right)^{2/3} \left(\frac{m_{\rm PBH}}{10^{-12} M_\odot} \right)^{5/3} \left(\frac{d_L}{1\ \text{kpc}} \right)^{-1}, \tag{15}$$

for a generic PBH. This is seen to be orders of magnitude lower than sensitivities $\text{Log}(\text{h}_0) \simeq -26$ at kilohertz frequencies planned for the next generations of detectors like CE with a sensitivity depth $D_{\rm s} = 20$–$30/\sqrt{\text{Hz}}$.

The technology required for an indirect detection is radically different and based in microwave cavities, so that a GW passing through a cavity containing a static magnetic field produces an effective current giving rise to an electromagnetic field that oscillates at the same frequency of the GW.

Ultrahigh-frequency GW in the gigahertz band would naturally be produced in other scenarios as well such as at the horizon size at grand unification or string scales and in phenomena like phase transitions and preheating after inflation as discussed in [82]. It would be difficult to detect with present sensitivities; we most likely could be able to detect such events only in the Milky Way or nearby satellite galaxies at distances of dozens of kiloparsecs.

IV. CONCLUSIONS AND DISCUSSION

We have argued that accumulation of sufficient, for example, asymmetric, DM inside a single NS may trigger the collapse into a low-mass BH, and this releases unique neutrino signals and possibly also ultrahigh-frequency GW signals in the ∼ gigahertz band. Such emission is not accessible with current interferometer devices and could be detected via future experiments based on resonant cavities. In addition to bosonic and fermionic ADM and self-annihilating candidates with feeble interactions with ordinary matter, there has been further recent discussion on PBH-NS accretion or collisional capture and the path of sink PBH material into the NS. Associated phenomena such as mechanisms for fast radio bursts (FRBs) warm up the inner core.

We do not address the source enigma of the FRB which is due to the reconnecting NS magnetic field (see [83]). Subsequently, FRBs and electromagnetic transients, such as kilonova-type afterglows, could occur during the collisions of PBH with NS following energy release via gravitational drag. These PBH-NS collisions are a probe of DM PBH-dominated galactic halos [84,85]. The light component, that is, an imploding solar mass NS, including the EOS in relativistic and nonrelativistic regimes [86], could play an important role in interpreting the trigger of a LIGO subsolar mass candidate. Simulations [87] of PBH capture by both NSs and strange stars show GW signal differences at kilohertz frequencies, potentially resembling our case of DM-induced collapse to a BH and suggesting that this might be a novel probe of the dense matter equation of state. Such collapsing NSs are candidates for FRBs [85,88].

We have focused here on the low-mass BH fate of these NSs. The neutrino luminosity curve obtained from our calculation shows a unique and much fainter character than for regular CCSN or NS-BH mergers. Strategies of detection based on coincidence signals from multimessengers seem very challenging with current technologies, although constraining the DM phase space may be within reach in the particular scenario of imploding NSs.

ACKNOWLEDGMENTS

Y. Z. was partially supported by NASA and Grant No. NNH17ZDA001N. C. A. and M. A. P.-G. acknowledge partial support from Junta de Castilla y León SA096P20 and Spanish Ministry of Science PID2019-107778GB-100 and PID2022-137887NB-100 projects.

[1] M. S. Athar, S. W. Barwick, T. Brunner, J. Cao, M. Danilov, K. Inoue, T. Kajita, M. Kowalski, M. Lindner, K. R. Long *et al.*, Prog. Part. Nucl. Phys. **124**, 103947 (2022).
[2] B. P. Abbott, R. Abbott, T. D. Abbott, F. Acernese, K. Ackley, C. Adams, T. Adams, P. Addesso, R. X. Adhikari, V. B. Adya *et al.*, Nature (London) **551**, 85 (2017).
[3] B. D. Metzger, Living Rev. Relativity **23**, 1 (2019).
[4] E. Nakar, Phys. Rep. **886**, 1 (2020).
[5] D. Radice, S. Bernuzzi, and A. Perego, Annu. Rev. Nucl. Part. Sci. **70**, 95 (2020).
[6] A. Hewish, S. J. Bell, J. D. H. Pilkington, P. F. Scott, and R. A. Collins, Nature (London) **217**, 709 (1968).
[7] F. Özel and P. Freire, Annu. Rev. Astron. Astrophys. **54**, 401 (2016).
[8] K. Chatziioannou and W. M. Farr, Phys. Rev. D **102**, 064063 (2020).
[9] S. Hild, M. Abernathy, F. Acernese, P. Amaro-Seoane, N. Andersson, K. Arun, F. Barone, B. Barr, M. Barsuglia, M. Beker *et al.*, Classical Quantum Gravity **28**, 094013 (2011).
[10] M. Evans, R. X. Adhikari, C. Afle, S. W. Ballmer, S. Biscoveanu, S. Borhanian, D. A. Brown, Y. Chen, R. Eisenstein, A. Gruson *et al.*, arXiv:2109.09882.
[11] F. Iacovelli, M. Mancarella, C. Mondal, A. Puecher, T. Dietrich, F. Gulminelli, M. Maggiore, and M. Oertel, Phys. Rev. D **108**, 122006 (2023).
[12] D. Barba-González, C. Albertus, and M. A. Pérez-García, Phys. Rev. C **106**, 065806 (2022).
[13] W. H. Press and D. N. Spergel, Astrophys. J. **296**, 679 (1985).
[14] A. Gould, Astrophys. J. **321**, 571 (1987).
[15] G. Bertone and D. Hooper, Rev. Mod. Phys. **90** (2018).
[16] G. Bertone, D. Hooper, and J. Silk, Phys. Rep. **405**, 279 (2005).
[17] K. Choi, S. H. Im, and C. S. Shin, Annu. Rev. Nucl. Part. Sci. **71**, 225 (2021).
[18] B. Carr and F. Kühnel, SciPost Phys. Lect. Notes (2022).
[19] B. Carr and F. Kuhnel, SciPost Phys. Lect. Notes **48**, 1 (2022).
[20] J. Bramante and T. Linden, Phys. Rev. Lett. **113**, 191301 (2014).
[21] B. Dasgupta, R. Laha, and A. Ray, Phys. Rev. Lett. **126**, 141105 (2021).
[22] S. Bhattacharya, B. Dasgupta, R. Laha, and A. Ray, Phys. Rev. Lett. **131**, 091401 (2023).
[23] C. B. Richards, T. W. Baumgarte, and S. L. Shapiro, Phys. Rev. D **103**, 104009 (2021).
[24] E. Fonseca *et al.*, Astrophys. J. Lett. **915**, L12 (2021).
[25] R. Abbott, T. D. Abbott, S. Abraham, F. Acernese, K. Ackley, C. Adams, R. X. Adhikari, V. B. Adya, C. Affeldt, M. Agathos *et al.*, Astrophys. J. Lett. **896**, L44 (2020).

[26] C. Y. Lam, J. R. Lu, A. Udalski, I. Bond, D. P. Bennett, J. Skowron, P. Mróz, R. Poleski, T. Sumi, M. K. Szymański *et al.*, Astrophys. J. Lett. **933**, L23 (2022).
[27] D. Singh, A. Gupta, E. Berti, S. Reddy, and B. S. Sathyaprakash, Phys. Rev. D **107**, 083037 (2023).
[28] R. Garani, D. Levkov, and P. Tinyakov, Phys. Rev. D **105**, 063019 (2022).
[29] I. Goldman and S. Nussinov, Phys. Rev. D **40**, 3221 (1989).
[30] S. D. McDermott, H.-B. Yu, and K. M. Zurek, Phys. Rev. D **85**, 023519 (2012).
[31] G. Defillon, E. Granet, P. Tinyakov, and M. H. G. Tytgat, Phys. Rev. D **90**, 103522 (2014).
[32] P. Montero-Camacho, X. Fang, G. Vasquez, M. Silva, and C. M. Hirata, J. Cosmol. Astropart. Phys. 08 (2019) 031.
[33] Y. Génolini, P. D. Serpico, and P. Tinyakov, Phys. Rev. D **102**, 083004 (2020).
[34] M. A. Perez-Garcia, J. Silk, and J. R. Stone, Phys. Rev. Lett. **105**, 141101 (2010).
[35] A. Herrero, M. A. Pérez-García, J. Silk, and C. Albertus, Phys. Rev. D **100**, 103019 (2019).
[36] M. Á. Pérez-García, F. Daigne, and J. Silk, Astrophys. J. **768**, 145 (2013).
[37] K. Kotera, M. A. Perez-Garcia, and J. Silk, Phys. Lett. B **725**, 196 (2013).
[38] M. Á. Pérez-García, K. Kotera, and J. Silk, Nucl. Instrum. Methods Phys. Res., Sect. A **742**, 237 (2014).
[39] G. M. Fuller, A. Kusenko, and V. Takhistov, Phys. Rev. Lett. **119**, 061101 (2017).
[40] J. Bramante and T. Linden, Astrophys. J. **826**, 57 (2016).
[41] B. E. Zhilyaev, Bulletin of the Crimean Astrophysical Observatory **103**, 58 (2007).
[42] M. A. Abramowicz, J. K. Becker, P. L. Biermann, A. Garzilli, F. Johansson, and L. Qian, Astrophys. J. **705**, 659 (2009).
[43] D. A. Perley, C. Fremling, J. Sollerman, A. A. Miller, A. S. Dahiwale, Y. Sharma, E. C. Bellm, R. Biswas, T. G. Brink, R. J. Bruch *et al.*, Astrophys. J. **904**, 35 (2020).
[44] W. E. East and L. Lehner, Phys. Rev. D **100**, 124026 (2019).
[45] N. K. Glendenning, *Compact Stars: Nuclear Physics, Particle Physics, and General Relativity* (Springer, New York, 1997).
[46] N. F. Bell, G. Busoni, S. Robles, and M. Virgato, J. Cosmol. Astropart. Phys. 09 (2020) 028.
[47] M. Mariani, C. Albertus, M. d. R. Alessandroni, M. G. Orsaria, M.Pérez-García, and I. F. Ranea-Sandoval, Mon. Not. R. Astron. Soc. **527**, 6795 (2023).
[48] C. Kouvaris, Phys. Rev. D **77**, 023006 (2008).
[49] M. Ángeles Pérez-García, H. Grigorian, C. Albertus, D. Barba, and J. Silk, Phys. Lett. B **827**, 136937 (2022).
[50] V. Takhistov, G. M. Fuller, and A. Kusenko, Phys. Rev. Lett. **126**, 071101 (2021).
[51] Y. Génolini, P. Serpico, and P. Tinyakov, Phys. Rev. D **102**, 083004 (2020).
[52] Z.-C. Zou and Y.-F. Huang, Astrophys. J. Lett. **928**, L13 (2022).
[53] M. Abramowicz, M. Bejger, A. Udalski, and M. Wielgus, Astrophys. J. Lett. **935**, L28 (2022).
[54] R. Abbott, H. Abe, F. Acernese, K. Ackley, S. Adhicary, N. Adhikari, R. X. Adhikari *et al.* (LIGO Scientific Collaboration, Virgo Collaboration, and KAGRA Collaboration), Mon. Not. R. Astron. Soc. **524**, 5984 (2023).
[55] A. Herrero, M. Pérez-García, J. Silk, and C. Albertus, Phys. Rev. D **100**, 103019 (2019).
[56] C. D. Ott, A. Burrows, T. A. Thompson, E. Livne, and R. Walder, Astrophys. J. Suppl. Ser. **164**, 130 (2006).
[57] Compact stars: Nuclear physics, particle physics, and general relativity (2000).
[58] E. O'Connor and C. D. Ott, Classical Quantum Gravity **27**, 114103 (2010).
[59] E. O'Connor and C. D. Ott, Astrophys. J. **730**, 70 (2011).
[60] Q. T. Ngo and S. Shinmura, Mod. Phys. Lett. A **32**, 1750190 (2017).
[61] A. S. Schneider, C. Constantinou, B. Muccioli, and M. Prakash, Phys. Rev. C **100**, 025803 (2019).
[62] M. Prakash, T. L. Ainsworth, and J. M. Lattimer, Phys. Rev. Lett. **61**, 2518 (1988).
[63] J. M. Lattimer and M. Prakash, Phys. Rep. **333**, 121 (2000).
[64] M. Ángeles Pérez-García, Eur. Phys. J. A **44**, 77 (2010).
[65] S. Chakraborty, P. Bhattacharjee, and K. Kar, Phys. Rev. D **89**, 013011 (2014).
[66] F. Hossein Nouri, M. D. Duez, F. Foucart, M. B. Deaton, R. Haas, M. Haddadi, L. E. Kidder, C. D. Ott, H. P. Pfeiffer, M. A. Scheel *et al.*, Phys. Rev. D **97**, 083014 (2018).
[67] D. G. Yakovlev and C. J. Pethick, Annu. Rev. Astron. Astrophys. **42**, 169 (2004).
[68] K. Abe, K. Haga, Y. Hayato, M. Ikeda, K. Iyogi, J. Kameda, Y. Kishimoto, M. Miura, S. Moriyama, M. Nakahata *et al.*, Astrophys. J. Lett. **830**, L11 (2016).
[69] K. Abe, C. Bronner, Y. Hayato, M. Ikeda, K. Iyogi, J. Kameda, Y. Kato, Y. Kishimoto, L. Marti, M. Miura *et al.*, Astrophys. J. Lett. **857**, L4 (2018).
[70] R. Abbasi, M. Ackermann, J. Adams, S. K. Agarwalla, J. A. Aguilar, M. Ahlers, J. M. Alameddine, N. M. Amin, K. Andeen, G. Anton *et al.*, Astrophys. J. **959**, 96 (2023).
[71] A. Albert *et al.* (ANTARES Collaboration), J. Cosmol. Astropart. Phys. 04 (2023) 004.
[72] A. Bauswein, N.-U. F. Bastian, D. B. Blaschke, K. Chatziioannou, J. A. Clark, T. Fischer, and M. Oertel, Phys. Rev. Lett. **122**, 061102 (2019).
[73] D. Lopez, S. Tiwari, M. Drago, D. Keitel, C. Lazzaro, and G. A. Prodi, Phys. Rev. D **106**, 103037 (2022).
[74] A. K. L. Yip, P. C.-K. Cheong, and T. G. F. Li, arXiv:2305.15181.
[75] T. Zhang, J. c. v. Smetana, Y. Chen, J. Bentley, D. Martynov, H. Miao, W. E. East, and H. Yang, Phys. Rev. D **103**, 044063 (2021).
[76] W. C. G. Ho, D. I. Jones, N. Andersson, and C. M. Espinoza, Phys. Rev. D **101**, 103009 (2020).
[77] Y. Kurita and H. Nakano, Phys. Rev. D **93**, 023508 (2016).
[78] B. Dasgupta, R. Laha, and A. Ray, Phys. Rev. Lett. **126**, 141105 (2021).
[79] S. Barsanti, V. De Luca, A. Maselli, and P. Pani, Phys. Rev. Lett. **128**, 111104 (2022).
[80] Y. Génolini, P. D. Serpico, and P. Tinyakov, Phys. Rev. D **102**, 083004 (2020).
[81] G. Franciolini, A. Maharana, and F. Muia, Phys. Rev. D **106**, 103520 (2022).

[82] N. Aggarwal, O. D. Aguiar, A. Bauswein, G. Cella, S. Clesse, A. M. Cruise, V. Domcke, D. G. Figueroa, A. Geraci, M. Goryachev *et al.*, Living Rev. Relativity **24**, 4 (2021).
[83] E. Petroff, J. W. T. Hessels, and D. R. Lorimer, Astron. Astrophys. Rev. **27**, 4 (2019).
[84] G. M. Fuller, A. Kusenko, and V. Takhistov, Phys. Rev. Lett. **119**, 061101 (2017).
[85] M. A. Abramowicz, M. Bejger, and M. Wielgus, Astrophys. J. **868**, 17 (2018).
[86] G. Morrás, J. F. Nuño Siles, A. Menéndez-Vázquez, C. Karathanasis, K. Martinovic, K. S. Phukon, S. Clesse, J. García-Bellido, M. Martínez, E. Ruiz Morales *et al.*, Phys. Dark Universe **42**, 101285 (2023).
[87] Z.-C. Zou and Y.-F. Huang, Astrophys. J. Lett. **928**, L13 (2022).
[88] K. Kainulainen, S. Nurmi, E. D. Schiappacasse, and T. T. Yanagida, Phys. Rev. D **104**, 123033 (2021).